Investigation of Formability, Morphology and Functionality of Chitosan based Biosensors

KANCHANA M*[1], JAYAPPRIYAN R M[1], KUMAR B[1] AND USHA ANTONY[2]

[1]. Department of Printing Technology, College of Engineering Guindy, Anna University, Chennai– 600 025, Tamil Nadu, India.

[2]. Centre for Food Technology, A.C. Tech., Anna University, Chennai– 600 025, Tamil Nadu, India.

ABSTRACT

Dilute solution of chitosan has been deposited on glass slide by inkjet printing and the efficacy of the coating for its formability, morphology and functionality has been explored. The chitosan coating was characterized by SEM, AFM, Optical Microscope and Spectrophotometer. The biosensor formulation (ferritin) entrapped between two layers of chitosan coating exhibited active functional characteristics confirming that chitosan coatings fabricated by inkjet printing could be utilized for optical biosensor applications.

Keywords: *Chitosan, Biopolymer, Surface coating, Inkjet Printing, Optical biosensors*

1. INTRODUCTION

Biosensors have a range of applications in many areas namely food processing and packaging, medical diagnosis, environmental monitoring, defence applications, storage and logistics, etc.[1–3] The biocompatibility and biodegradability of the biosensors makes them highly desirable in the food and medical industry. Chitosan, a linear polysaccharide, obtained from deacetylation of chitin is one of the extensively used materials in biosensor applications. It is composed of randomly distributed β-(1→4)-linked D-glucosamine (deacetylated unit) and *N*-acetyl-D-glucosamine (acetylated unit) [4,5]. Chitosan has free amino groups and its reactivity, mechanical and barrier property could be enhanced by adding other polymers, nanomaterials, and biomolecules [6]. It can be used for developing optical biosensors due to its excellent film forming ability, permeability, optical transparency and capacity to physically entrap and chemically immobilize bio-molecules[7]. Chitosan based optical biosensors have been reported to detect copper

J. Polym. Mater. Vol. **34,** No. 4, 2017, 747-758

Correspondence author e-mail: mani.kanchana@gmail.com

ions [8], cadmium ions[9], mercury ions [10], catechol [11], hydrogen sulphide gas [12], and ammonia gas[13].

For producing biosensors, chitosan is deposited as a thin film in a specific pattern. Thin film chitosan depositions are generally fabricated by spin coating, nanoimprinting, microcontact printing and electrodeposition [7]. Spin coating technique is not practically suitable for large scale manufacturing [14]. Thermolithography [15] or photolithography[16] are used as additional steps to create patterns on the casted films. Electrodeposition is suitable for forming spatially and temporally patterned chitosan coatings on planar and non-planar surfaces [17–19]. Nanoimprint lithography involves heat and pressure to pattern the chitosan into nanostructures[20,21]. Microcontact printing involves inking a poly(dimethylsiloxane) stamp made by photolithography and transferring the chitosan solution to a substrate by pressure. Many of the above techniques require a mold or mask to create patterns. Moreover direct contact, heat, impact or UV curing are some of the disadvantages in these processes.

Non-impact inkjet printing technology, offers a simple, low cost, high throughput alternate method for deposition of liquids in microscale level with complex patterns. It does not require any masking step and very small volumes of material can be deposited [2,22,23]. It is also possible to simultaneously fabricate more than one material at a time and commercial inkjet heads could be integrated with production line to print the biosensors directly on packaging materials. Feasibility of thin chitosan coatings by drop-on-demand piezoelectric inkjet printing for biosensor applications is not widely reported. In the present work, chitosan was deposited on glass substrate by piezoelectric inkjet printing. The bipolar waveform parameters for drop generation were optimized and the resultant coating was investigated for morphological properties using SEM, AFM and Optical Microscope. The functional material (ferritin) was entrapped between two layers of chitosan and their efficacy with respect to optical and colorimetric properties were analysed using Spectrophotometer. The results were highly encouraging.

2. MATERIALS AND METHODS

2.1 Materials

Low molecular weight Chitosan (viscosity 20-300 cPs in 2% acetic acid) was purchased from CDH, India. Ferritin from equine spleen was purchased from Sigma Aldrich (USA). Acetic acid glacial was purchased from Merck (India).

2.2 Preparation of chitosan solution

Chitosan solution was prepared by adding 0.25 g of chitosan to 50 mL of de-ionized water containing 0.5 mL of acetic acid [24]. The mixture was stirred at room temperature in a magnetic stirrer for 4 hours. The solution was further kept in a sonicator for 2 hours at room temperature[25]. The viscosity of the polymer solution was measured in Anton Paar MCR 302 Rheometer (Germany) using a cone and plate system. The surface tension of the solution was measured with Kyowa Surface Tensiometer DY300 (Japan) and the contact angle was measured with Kyowa DMs-200 (Japan) contact angle meter.

2.3 Preparation of glass slides

Prior to printing, the surface of the glass slides were treated with dilute hydrochloric acid for better adhesion of the coating and rinsed in distilled water. Further the slides were immersed in ethanol and kept in an ultrasonic bath for 15 minutes to remove any impurities present on the surface. The same procedure was repeated with acetone and isopropanol and finally dried in a hot plate at 200°C.

2.4 Inkjet printing

Microfab Jetlab 4XL Inkjet printer (USA) (Fig 1) was used for deposition of chitosan and protein solutions. Jetlab is a drop-on-demand piezoelectric inkjet printer that has a fixed printhead and movable substrate holder. The movement of the substrate holder can be controlled in the X, Y and Z directions. The printhead assembly consists of a reusable reservoir and is connected to the print head by PTFE tubing. The print head has a glass capillary tube with an integrated orifice in the range of 20 - 80 µm and an annular piezoelectric transducer attached to it. The horizontal stroboscopic camera is used for observing the drop formation and vertical camera is used for fiducial image positioning. The fluid in the printhead assembly is controlled pneumatically and the printhead signal is controlled by JetDrive™ V drive electronics. A bipolar waveform applied to the piezoelectric transducer controls the drop formation process. When the voltage is increased from zero to higher level, the fluid chamber expands causing a negative pressure wave. The positive voltage is maintained for a particular duration of time (dwell time) allowing the pressure wave to propagate inside the chamber. When the voltage level falls, the fluid chamber is compressed and the fluid is ejected from the orifice at high velocity. The negative echo voltage is used to cancel the residual acoustic waves inside the tube [26].

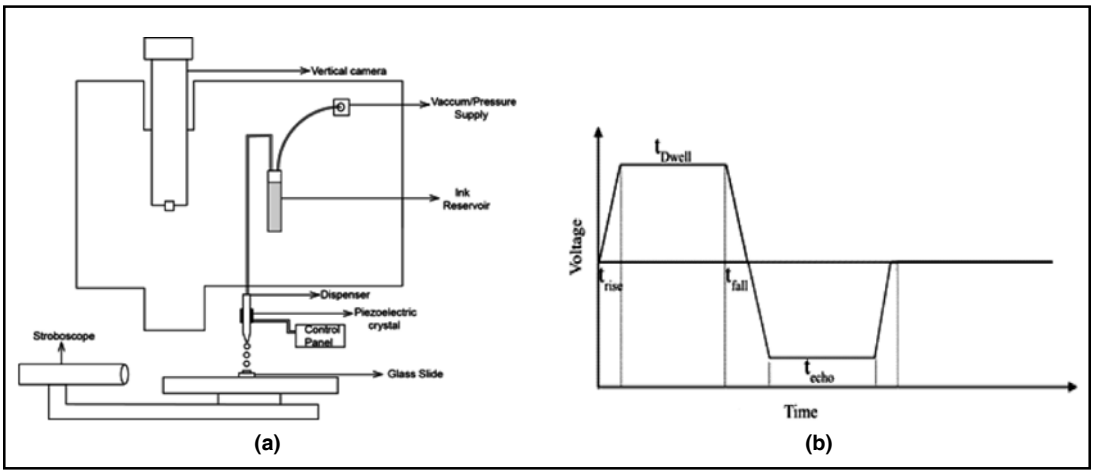

Fig. 1(a) Schematic diagram of Microfab Jetlab 4XL printer (b) Bipolar waveform

Printing was carried out with 60 µm nozzle on glass microscope slides after thorough cleaning. Before printing, the chitosan solution was filtered using 0.22 µm syringe filter and was filled in the 2 mL reservoir. Printing was carried out in three different resolutions of 0.50 mm, 0.25 mm, and 0.10 mm. After identifying the optimum resolution, chitosan was deposited in three different glass slides as single layer, double layer and triple layer coating. The various printed layer patterns are shown in Fig 2.

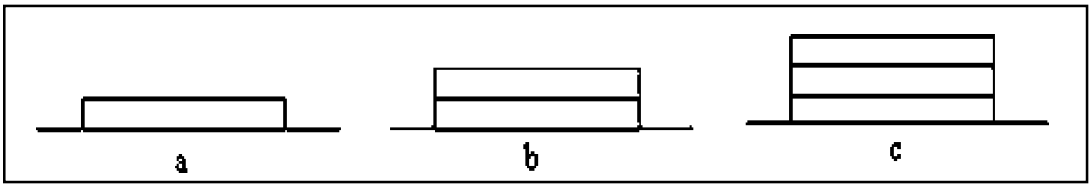

Fig. 2 Printed layer patterns of chitosan a) Single layer b) Double layer c) Triple layer

2.5 Encapsulation of ferritin for biosensor application

Ferritin is an iron storage protein, used widely in biosensor applications. In this work, ferritin was physically trapped between two layers of chitosan by inkjet printing. After printing a single layer of chitosan, a layer of ferritin was printed followed by another layer of chitosan. The entrapped ferritin was tested for its functionality by placing it in a gas tight bottle and passing hydrogen sulphide gas.

2.6 Process optimization and characterization

The jettability of the chitosan solution was analysed by observing the jetted drops through the inbuilt Navitar camera. The consistency of the printing with respect to the structure of the printed drop was analysed with Scanning Electron Microscope (Hitachi S3400N). The layer structures were investigated with Carl Zeiss Primo Vert inverted optical microscope and the images were recorded with AxioCam ERc 5s camera. The surface morphology of the coating was characterized using Atomic Force Microscope (Park XE-100). The optical and colorimetric properties of the coating were characterized by Techkon Spectrodens Premium.

3. Optimizing Jettability Parameters

The viscosity and surface tension of the dilute chitosan solution were 20 cP and 55.13 mN/m respectively. The contact angle of the chitosan solution (Fig 3) on the glass plate was 24^{o} indicating that the wettability is good.

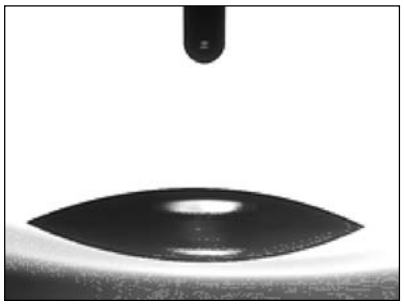

Fig 3. Contact angle of chitosan solution on glass slide

3.1 Drop Formation

The formation of drops in a piezoelectric inkjet head is influenced by vacuum level held in the reservoir, frequency and shape of the waveform applied to actuate the head [27]. The waveform parameters should be optimised to get consistent drops preferably without satellite drop formation. The vacuum level and waveform parameters used for jetting chitosan are given in Table 1. The formation and the trajectory of the drop were observed by the stroboscopic camera in the Jetlab printing system. Aphelion image analysis software was used to analyse the jetted drop and the jetting velocity, drop volume and drop diameter, which are tabulated in Table 2.

TABLE 1. Bipolar waveform parameters

Solution	Rise time1 (in µs)	Dwell time (in µs)	Fall time (in µs)	Echo time (in µs)	Rise time 2 (in µs)	Idle Voltage (in V)	Dwell Voltage (in V)	Echo Voltage (in V)	Frequency (in Hz)	Vacuum level (in kPa)
Chitosan	4	72	6	72	3	0	54	-54	850	1.6

TABLE 2. Drop analysis values

	Jetting velocity (in m/s)	Drop volume (in pL)	Drop diameter (in µm)
Chitosan Solution	1.71	194	71.85

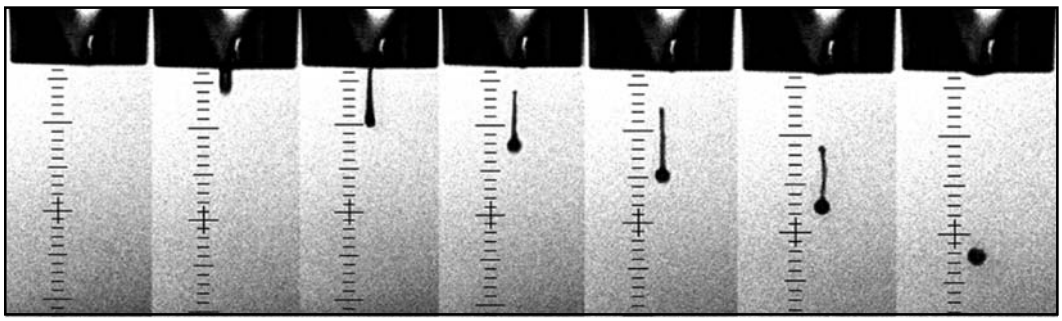

Fig. 4. Ejection of chitosan and drop formation

The drop formation process of chitosan is shown in Fig 4 and a long tail attached to the main drop can be observed. The tail later pinches-off from the liquid and gets attached to the main drop before being deposited on the glass substrate. This is similar to the drop formation observed for dilute polymer solutions[28].

3.2 Drop uniformity

A two dimensional grid with a drop spacing of 0.25 mm was printed to analyze the uniformity of the jetted drops. The SEM image was used to investigate the printed pattern of the chitosan coating (Fig. 5. a). The area, perimeter, major axis and minor axis of the printed drops

TABLE 3. Drop parameters measured in Image J software

Sample No.	Area in mm^2	Perimeter in mm	Major axis in mm	Minor axis in mm
1	0.010	0.358	0.117	0.112
2	0.013	0.402	0.129	0.129
3	0.012	0.390	0.124	0.124
4	0.013	0.402	0.132	0.125
5	0.008	0.314	0.104	0.096
6	0.012	0.396	0.128	0.124
7	0.011	0.377	0.124	0.117
8	0.011	0.371	0.125	0.112
9	0.012	0.383	0.124	0.119
10	0.012	0.390	0.124	0.124
11	0.011	0.371	0.121	0.117
12	0.011	0.364	0.116	0.116
13	0.011	0.364	0.121	0.113
14	0.011	0.371	0.125	0.112
Mean	**0.011**	**0.375**	**0.122**	**0.117**
SD	**0.001**	**0.023**	**0.007**	**0.008**

were evaluated using ImageJ software (Fig. 5. b) and tabulated in Table 3. The mean area of the drops were 0.011 mm^2 (SD - 0.001) and the difference between the mean of major and minor axes were 0.005 mm.

3.3 Drop Spacing

The optical microscope images of the drop patterns printed at drop spacings of 0.50 mm, 0.25 mm, 0.10 mm and 0.05 mm is shown in Fig. 6. It is observed that there was a gap between the drops for interdrop spacing of 0.50 mm and 0.25 mm. The drops join and form a uniform thin line with neat edges for the drop spacing 0.10 mm. For 0.05 mm, the drops overlap to form an edge with a thick layer. Drop spacing of 0.10 mm will be suitable for forming micro-level patterns and drop spacing of 0.05 mm will be suitable for forming a coating.

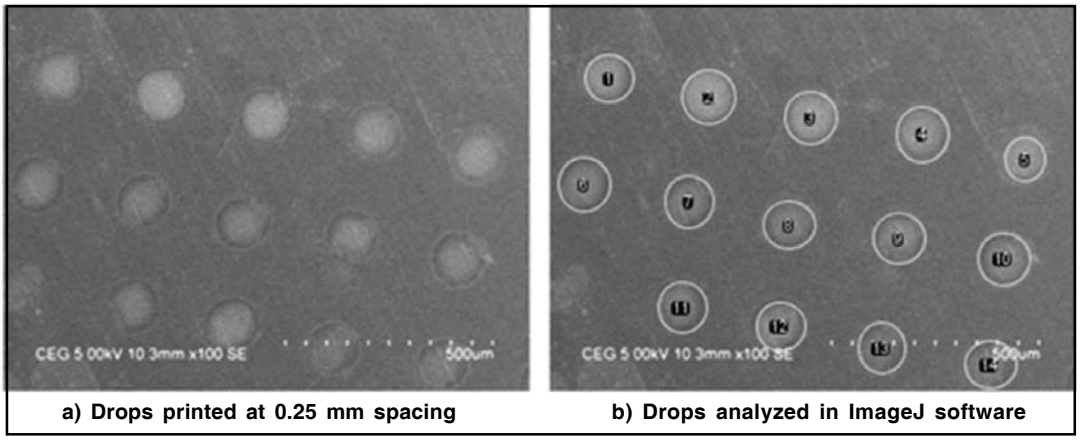

Fig. 5. SEM images of the chitosan printed pattern.

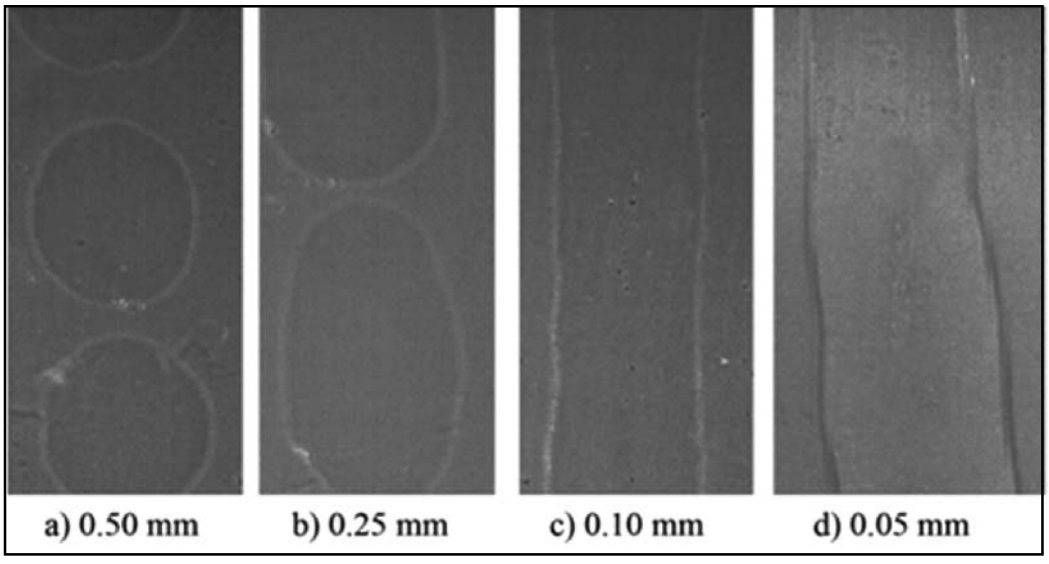

Fig. 6. Optical microscope image of printed pattern at different drop spacing

4. RESULT AND DISCUSSION

4.1 Analysis of layer patterns

A square pattern was printed with chitosan solution as single layer, double layer and triple layer with a drop spacing of 0.05 mm. From the single layer image (Fig. 7. a), it could be observed that the drops have merged in the vertical direction and not in the horizontal direction leading to striations. The two dimensional pattern was created by printing an array of vertical lines. The adjacent drops in the vertical direction were wet and hence merged together. By the time, the printhead completed the first vertical line and started to print the second line again from the top, the drop edges in the first line were dry and hence did not merge with the second line. In the double layer printed image (Fig. 7. b), the gap between the lines were still visible, but the drops merged better and the lines appear as ridges. In the triple layer printed image (Fig. 7. c), the coalesced drops resulted in a periodic pattern. Subsequently, the edges were more ragged and the bottom layers could be seen near the edges.

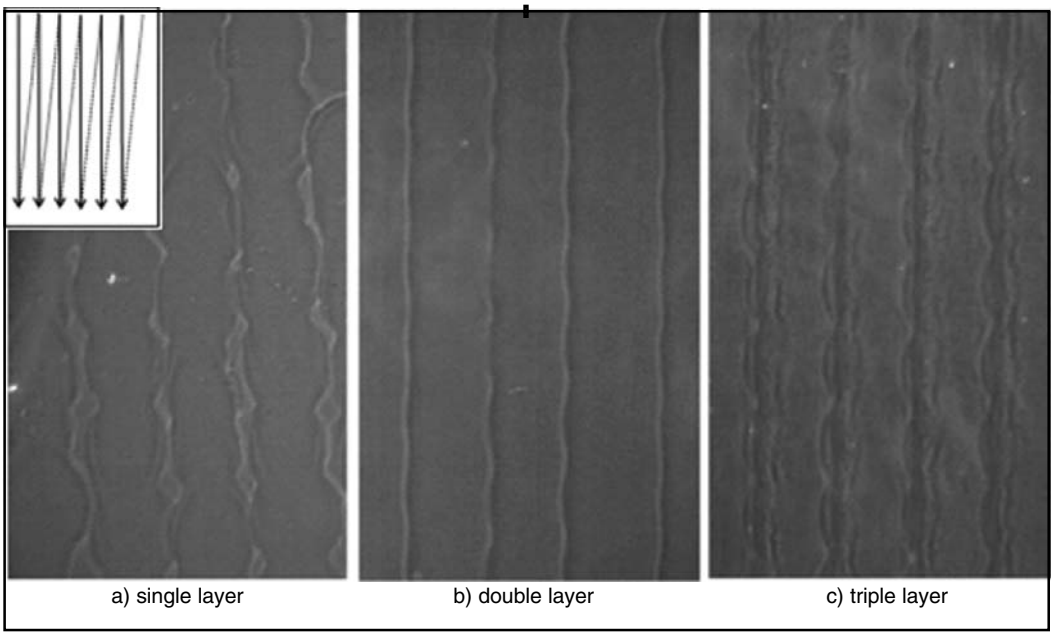

Fig. 7. Optical microscope image of printed layers (Inset - Print direction)

4.2 Surface morphology

The surface morphology of single layer, double layer and triple layer chitosan coating was analyzed using AFM under non-contact mode in a scan area of 15 μm x 15 μm (Fig. 8). The single layer and double layer depositions were more uniform than the triple layer coating confirming the image pattern obtained by optical

microscope. The roughness of the glass slide, single layer, double layer and triple layer chitosan coatings were plotted in Fig 9. The surface roughness of the dilute HCl acid activated glass slide was 0.738 nm and it could be observed that the single layer coating (roughness - 0.732 nm) took the surface profile of the glass surface. The second layer coating (roughness - 0.481 nm) slightly reduced the roughness of the surface. However, the third

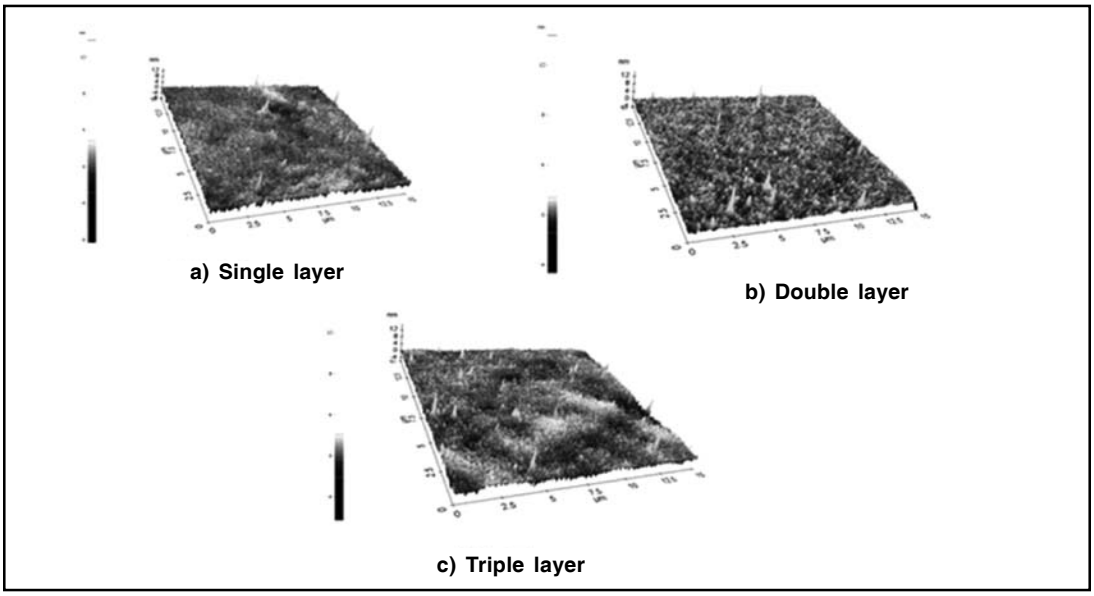

Fig. 8. AFM images of chitosan printed layers

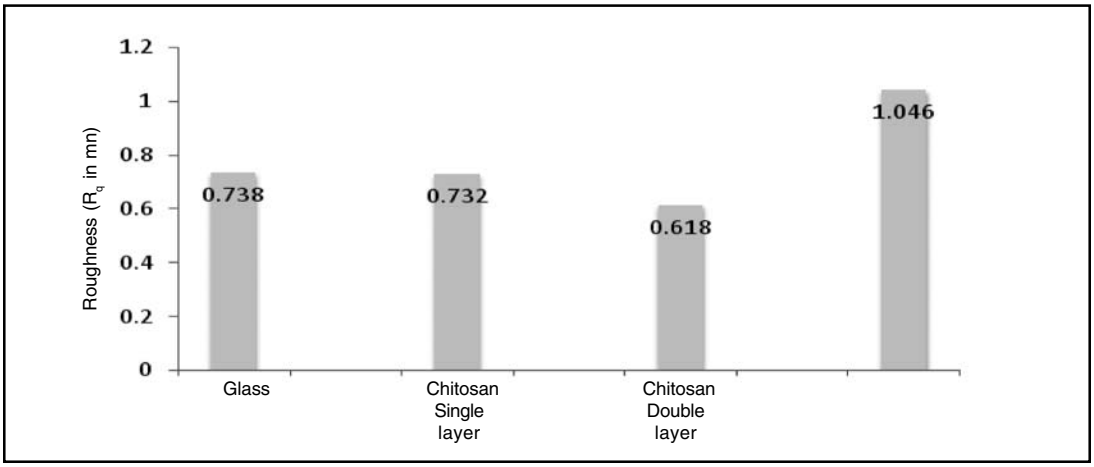

Fig. 9. Roughness values of chitosan layers

layer coating (roughness - 1.046 nm) showed increased roughness value due to the formation of undulations in the surface. Overall, the roughness of the chitosan coating was approximately 1 nm which is very less.

4.3 Optical properties

The optical properties of the chitosan coatings were measured with Spectrophotometer. The opacity and the L*a*b* values of the three coatings and plain glass are listed in Table 4. The colour difference between the glass slide and the chitosan coatings were computed using ΔE equation, ($\Delta E = \sqrt{(L^*_1 - L^*_2) + (a^*_1 - a^*_2)^2 + (b^*_1 - b^*_2)^2}$)] and it is observed that the colour difference is negligible as they are less than the perceptible colour difference value of 1[28]. The opacity values of the chitosan coatings were similar to that of glass as the coatings were transparent.

TABLE 4. Optical properties of chitosan coating

		Chitosan coating		
	Glass slide	Single layer	Double layer	Triple layer
L*	86.76	86.56	86.95	87.13
a*	-0.48	-1.21	-0.43	-0.27
b*	-7.55	-7.56	-7.51	-7.62
ΔE	—	0.77	0.21	0.43
Opacity in %	2.10	2.10	2.12	2.13

4.4 Functionality of ferritin entrapped in chitosan

The SEM image (Fig. 8) shows ferritin printed as an intermediate layer between two layers of chitosan. After printing, the slide was kept in a 60ml air tight chamber and different concentrations of hydrogen sulphide gas was passed into it to check whether entrapped ferritin reacted with the gas. The L*a*b* values and ΔE values are listed in Table 5. It was observed that ferritin retained its functionality even after entrapment and there was a visible colour change (Fig. 10) as indicated by the value of $\Delta E > 5$ which indicates a distinct colour

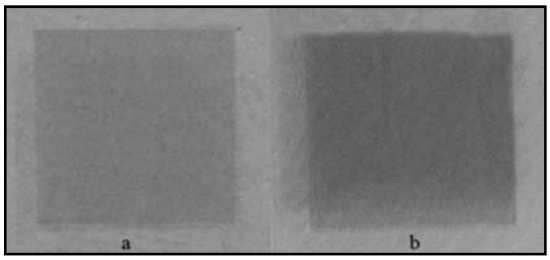

Fig 10. Image of ferritin entrapped between chitosan layers
a) Before reaction b) After reaction

difference [29]. The spectral reflectance values of the ferritin entrapped between the chitosan layers before and after reaction (Fig. 11) depicts a decrease in reflectance and increase in opacity and thereby enhancing the contrast. The entrapped ferritin displays a change in spectral reflectance for 0.1 mL increase in concentration of hydrogen sulphide gas. The ability of the sensor to regenerate was tested by passing 5 mL of hydrogen sulphide gas and after 5 minutes of reaction time, the printed sensor was exposed to normal atmosphere. Reflectance values were measured in regular intervals and it was observed that there was a significant change in the reflectance values in the initial 15 minutes after which the change was slower. The sensor retained its original colour approximately after 2.5 hours. (Fig. 12.)

TABLE 5. Colour values of entrapped ferritin

H2S concentration	**L***	**a***	**b***	**∆E**
0.0 mL	76.48	3.96	30.97	—
0.1 mL	72.82	3.68	25.23	6.81
0.2 mL	73.05	3.73	25.02	6.87
0.3 mL	73.52	3.86	24.63	7.00

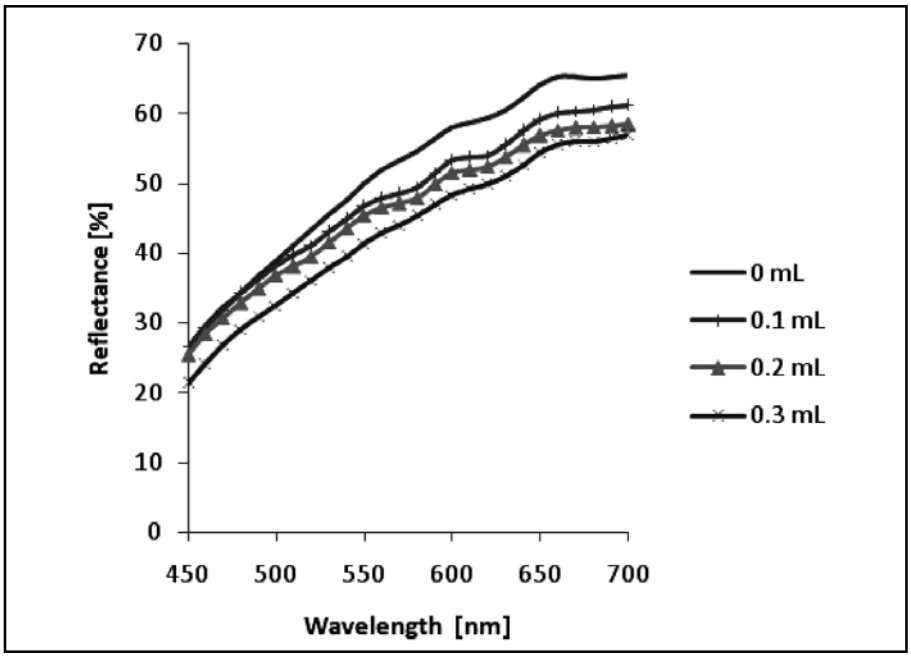

Fig. 11. Spectral reflectance values of entrapped ferritin with different concentrations of hydrogen sulphide gas.

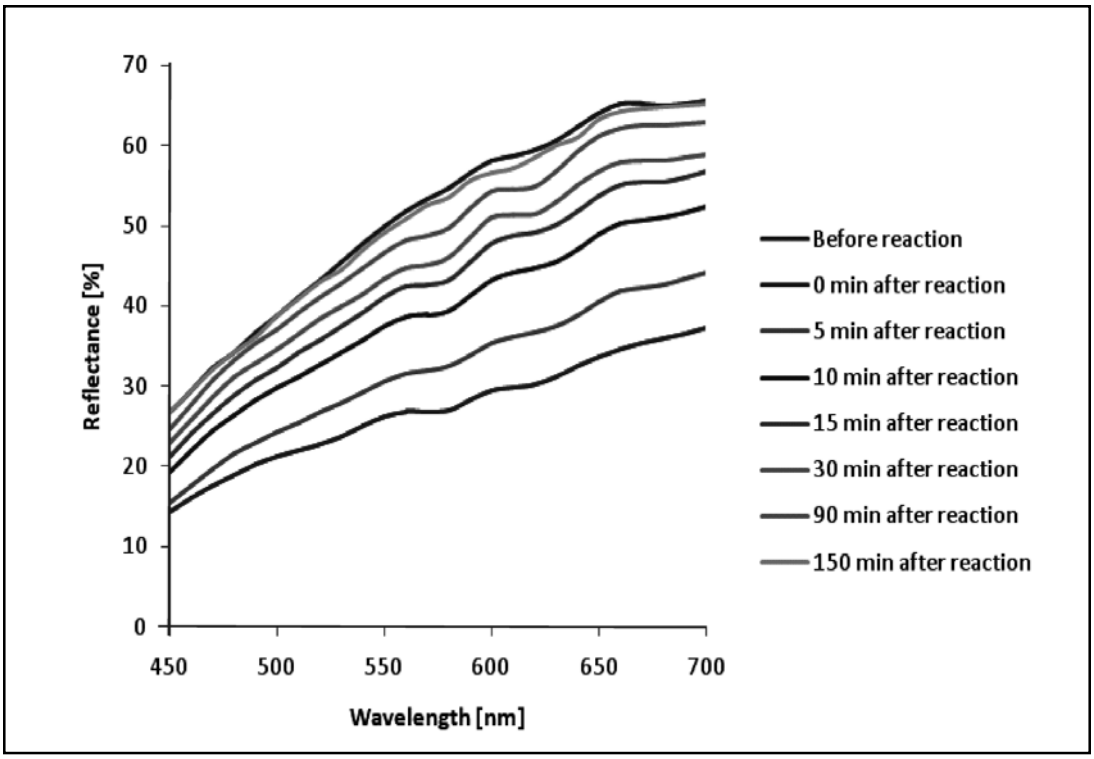

Fig. 12. Spectral reflectance values of entrapped ferritin showing regeneration of the sensor approximately after 2.5 hours.

4. CONCLUSION

The consistency of chitosan deposition by inkjet printing is proven to be good as is confirmed by SEM analysis. The inkjet deposited chitosan layers are extremely transparent making it ideal for applications in the field of optical biosensors. The smoothness of chitosan layers is good as is revealed from the roughness measurements obtained by AFM. The optical and spectral values obtained proves that the ferritin entrapped between chitosan layers retained the functional properties and allowed the hydrogen sulphide gas to permeate through it to react with ferritin to result into a distinct colour change.

Acknowledgement

The authors are grateful to the Department of Biotechnology, Ministry of Science and Technology, Government of India for funding the project. The authors are thankful to Centre for Biotechnology and Centre for Food Technology, Anna University for extending the research facilities and supporting the project work. Authors also thank the Department of Mechanical Engineering, College of Engineering, Guindy and Centre for Crystal Growth, Anna University, Chennai, for providing SEM and AFM facilities.

REFERENCES

1. Mehrotra, P. *J. Oral Biol. Craniofacial Res.* **6,** 153–159 (2016).
2. Dias, A. D., Kingsley, D. M. & Corr, D. T. *Biosensors* **4,** 111–136 (2014).
3. Turner, A. P. F. *Chem. Soc. Rev.* **42,** 3184 (2013).
4. Kumar Dutta, P., Dutta, J. & Tripathi, V. S. *J. Sci. Ind. Res.* **63,** 20–31 (2004).
5. Islam, S., Bhuiyan, M. A. R. & Islam, M. N. *J. Polym. Environ.* **25,** 854–866 (2017).
6. Cheung, R. C. F., Ng, T. B., Wong, J. H. & Chan, W. Y. *Marine Drugs* **13,** (2015).
7. Koev, S. T. *et al. Lab Chip* **10,** 3026 (2010).
8. Lin, S., Chang, C. C. & Lin, C. W. *Biomed. Eng. - Appl. Basis Commun.* **24,** 453–459 (2012).
9. Yulianti, I., P, N. M. D., Saputra, B. A., Mahardika, P. A. & Kurdi, O. Chitosan Layer Fabry-Perot Interferometer- Based Optical Fiber Sensor for Cadmium Ion Detection. 10–12 (2016).
10. Moksin, M. M., Talib, Z. A. & Yusof, N. O. R. A. *J. Optoelectron. Adv. Mater.* **13,** 279–285 (2011).
11. Dykstra, P. *et al. Sensors Actuators, B Chem.* **138,** 64–70 (2009).
12. Mironenko, A. Y. *et al. Sensors Actuators B Chem.* **225,** 348–353 (2016).
13. Mironenko, A. Y. *et al. Prog. Chem. Appl. Chitin its Deriv.* **22,** 159–165 (2017).
14. Zakir Hossain, S. M. *et al. Anal. Chem.* **81,** 5474–5483 (2009).
15. Wu, L.-Q. *et al. Langmuir* **19,** 519–524 (2003).
16. Pisano, J. C. C./ ; A. P. *J. Microelectromechanical Syst.* 402–409 (2008).
17. Geng, Z. *et al. J. Mater. Chem. B* **4,** 3331–3338 (2016).
18. Li, Y., Pang, X., Epand, R. F. & Zhitomirsky, I. *Mater. Lett.* **65,** 1463–1465 (2011).
19. Pang, X. & Zhitomirsky, I. *Mater. Chem. Phys.* **94,** 245–251 (2005).
20. Albert, P. & Sensor, B. *Image (Rochester, N.Y.)* 19997
21. Park, I., Cheng, J., Pisano, A. P., Lee, E.-S. & Jeong, J.-H. *Appl. Phys. Lett.* **90,** 93902 (2007).
22. Gonzalez-macia, L., Morrin, A., Smyth, M. R. & Killard, A. J. Advanced printing and deposition methodologies for the fabrication of biosensors and biodevices. 845–867 (2010). doi:10.1039/b916888e
23. Derby, B. & Derby, B. Bioprinting/ : Inkjet Printing Proteins and Hybrid Cell-Containing Materials and Structures Bioprinting/ : inkjet printing proteins and hybrid cell-containing materials and structures. 1–6 (2017). doi:10.1039/B807560C
24. Seshadri, V. Exploring the potential of Inkjet printing for the fabrication of tissue test systems. (2011).
25. Kasaai, M. R., Arul, J. & Charlet, G. *Ultrason. Sonochem.* **15,** 1001–1008 (2008).
26. Bogy, D. B. & Talke, *Ibm J. Res. Dev.* **28,** 314–321 (1984).
27. Thesis, D. *polyvinylalkoholu pro inkoustový tisk. (2017).*
28. Ohta, N. & Robertson, A. R. *Colorimetry: Fundamentals and Applications*. *Colorimetry: Fundamentals and Applications* (2006). doi:10.1002/0470094745
29. Souza, J. M. *et al. Brazilian J. Pharmacogn.* **24,** 691–698 (2014).

Received: 10-10-2017

Accepted: 25-12-2017